Desalination and Water Treatment
www.deswater.com
doi: 10.1080/19443994.2014.892031

54 (2015) 1684–1693
May

Taylor & Francis
Taylor & Francis Group

Adsorptive removal of vinyl polymer/ZnO nanocomposite from aqueous solution by activated sludge biomass

Xia Zhao[a], Hongrui Ma[b,*], Jianzhong Ma[b], Dangge Gao[b], Lizhen Hu[b], Xiangfei Lv[b]

[a]*College of Chemistry and Chemical Engineering, Shaanxi University of Science and Technology, Xi'an 710021, P.R. China*
[b]*College of Resources and Environment, Shaanxi University of Science and Technology, Xi'an 710021, P.R. China,*
Tel. +86 29 86168291; Fax: +86 29 86168291; email: mahr@sust.edu.cn

Received 23 August 2013; Accepted 25 January 2014

ABSTRACT

In this study, the removal potential of vinyl polymer/ZnO nanocomposite (PDM/ZnO) by activated sludge (AS) biomass was investigated. PDM/ZnO was effectively removed by AS adsorption (90.3% of total PDM/ZnO removed). The effects of contact time, temperature, pH of the solution, PDM/ZnO production method, initial adsorbate concentration, and properties of the adsorbent were studied. The experimental results are fitted with the Langmuir and Freundlich equations. The adsorption kinetics closely followed the pseudo-second-order model. Thermodynamic parameters (ΔH°, ΔS°, ΔG°) indicate that the adsorption of PDM/ZnO onto AS was feasible, spontaneous, and endothermic. The effects of PDM/ZnO production method and pH value both indicate that electrostatic force may main mechanism in PDM/ZnO adsorption process. The decrease in the adsorption capacity of inactivated sludge suggests that the increase of adsorbent surface area also plays a significant role in the removal process.

Keywords: Adsorption; Vinyl polymer/ZnO nanocomposite; Activated sludge

1. Introduction

With the rapid development of nanotechnology, nanoparticles, and materials have attracted a great deal of attention in recent years [1,2]. ZnO nanomaterials have been widely used in many fields such as sunscreens, electrical and optical devices, catalysts, food additives, biosensors, and industrial coatings [3–5]. Naturally occurring ZnO nanomaterials are also ubiquitous in the environment, resulting from both natural processes and from anthropogenic impacts. Despite the outstanding characteristics, many studies showed the potential toxicity of ZnO nanomaterials to the environment. Nano-ZnO has been found to be toxic to micro-organisms [2,6,7], fish [8], and plants [9,10] at various levels. Quantifying the affinity of nanomaterials for activated sludge (AS) is an essential step towards predicting its fate in the environment and assessing exposure risks [11].

Dimethyl diallyl ammonium chloride is a kind of water-soluble cationic monomer with non-conjugated diolefine which causes homopolymerization and copolymerization reactions. It has been extensively used in oilfields, papermaking, water treatment, leather making, textile printing and dyeing, medicine, cosmetics, etc. [12–14]. Vinyl polymer (dimethyl diallyl ammonium chloride/acrylic acid/2-hydroxyethyl acrylate/acrylamide) consists of numerous functional

*Corresponding author.

groups, such as –OH, –COOH, and –$CONH_2$. Organic-inorganic nanocomposite materials could combine the properties of organic and inorganic materials, so the mechanical, thermal, and other properties of the composite could be greatly improved [15]. Vinyl polymer/ZnO nanocomposite (PDM/ZnO) could combine the properties of the individual constituents and broaden its application range [16]. However, the transformation and fate of nano-ZnO may vary greatly with its chemical composition and molecular structure. In consideration of the potential toxicity and environmental impact of ZnO nanoparticles, it is necessary to evaluate PDM/ZnO nanocomposite entering wastewater treatment plants, and methods are needed for the industry to assess the potential removal of them during wastewater treatment.

AS is used to reduce concentrations of nutrients, suspended solids, metals, synthetic organic chemicals, and pathogens in wastewater [17]. Pollutants in AS processes can be removed through different mechanisms such as biodegradation, volatilization, air stripping, and adsorption [18]. Among these, adsorption on AS flocs is often the most important mechanism [19,20]. United States Environmental Protection Agency (USEPA) provided a standard method for testing soluble pollutant sorption on AS with the publication of the OPPTS 835.1110 [21], which calls for the use of freeze-dried and heat-treated (FDH) AS as an adsorbent. Unlike fresh AS, FDH AS can be stored for several months, allowing for a convenient and uniform supply of sorbent for batch experiments. However, research has shown that the use of FDH AS is inappropriate for quantifying nanoparticle removal in wastewater treatment plants [11]. Studies have been published that investigated the fate of manufactured nanoparticles (TiO_2, SiO_2, silver, gold, and fullerene nanoparticles) in wastewater treatment plants through AS [11,17], while very few related studies are available about ZnO nanocomposite.

The overall aim of this study was to explore the feasibility of using wastewater biomass as an effective adsorbent for the removal of PDM/ZnO nanocomposite. PDM/ZnO removal by AS and inactivated sludge (IAS) was compared with batch experiments. The effects of the solution pH, contact time, temperature, PDM/ZnO production method, initial adsorbate concentration, and properties of the adsorbent were also investigated. The accomplishment of these objectives will elucidate potential pathways for evaluating PDM/ZnO nanocomposite removal from wastewater and have important implications for the transformation and fate of PDM/ZnO nanocomposite in the environment.

2. Experimental procedures

2.1. Materials and analytical methods

PDM/ZnO nanocomposite was prepared by following our previous study [16]. I-PDM/ZnO was synthesized via *in situ* polymerization. Sodium azide (NaN_3) was purchased from Zhengzhou Paini Chemicals Co., Ltd (China). Other chemicals were supplied by Chinese chemical companies. All the chemicals were of analytical grade and were used without further treatment.

AS was taken from an aeration basin of a local municipal wastewater treatment plant, Xi'an, China. The sludge was acclimatized in the laboratory and was continuously aerated. The AS was fed with nutrients consisting of NH_4Cl, KH_2PO_4, and glucose. During the steady state, mixed liquor suspended solids (MLSS) concentration was approximately 4,090 mg/L. To investigate the effect of physicochemical properties of the adsorbent on the PDM/ZnO adsorption behavior, we added 1% NaN_3 as described by the previous studies [22–24] to make the AS inactivated. Sludge inactivation was controlled by monitoring the oxygen concentration. The inactivation of the AS was successful when no oxygen consumption took place [25].

Solid samples were observed using brightfield by an epifluorescence microscope (OPTPro BK-FL). The surface morphologies of AS and IAS were characterized by a scanning electron photomicrograph (SEM, Apollo XL) which is equipped with an EDX analyzer. Infrared spectra were recorded on a Vector-22 FTIR spectrometer with KBr pellet technology. Size distribution analysis was carried out using a Malvern Zetasizer Nano ZS90. Zeta potentials were measured using a Malvern Zeta Potential Analyzer. The surface areas of AS and IAS were characterized by Quantachrome NovaWin instruments with N_2 adsorption.

2.2. Batch adsorption procedure

A series of experiments included contact time, pH, temperature, and adsorbate concentration effects were conducted. The purpose was to investigate the kinetics, thermodynamics, and mechanisms of nanocomposite adsorption by AS. For the experimental determination of the required contact time, AS was added to a 250 mL conical flask at MLSS concentration of 1,000 mg/L and PDM/ZnO of approximately 400 mg/L concentration at pH 7.0 was obtained; the mixture was placed in an incubator operated at 120 rpm and 25°C. Samples were withdrawn at regular time intervals and the solutions were filtrated in order to remove any adsorbent particles. The filtrate

concentrations of PDM/ZnO were measured by a UV spectrophotometer (UV7200). The adsorption amounts of PDM/ZnO on adsorbent were calculated according to Eq. (1) [26]:

$$q_e = \frac{(C_0 - C_e)V}{M} \quad (1)$$

where q_e (mg/g) is the amount of PDM/ZnO adsorbed at equilibrium, C_0 is the initial concentration of PDM/ZnO (mg/L), C_e is the equilibrium PDM/ZnO concentration (mg/L), V is the volume of PDM/ZnO solution (L), and M is the adsorbent mass (g).

Effect of solution pH on PDM/ZnO adsorption on AS was studied and the pH values were adjusted from 3 to 12 with 0.1 mol/L HCl or 0.1 mol/L NaOH solutions. The procedures for the determination of the effect of pH were similar to those for the determination of the adsorption equilibrium time.

Adsorption isotherms at 15, 25, and 35°C were conducted as follows: AS was added to a 100 mL conical flask at MLSS 1,000 mg/L, then PDM/ZnO was added with concentrations approximately from 50 to 600 mg/L. The flasks were transferred into an incubator and shaken at 120 rpm and constant temperature for 30 min. After reaching adsorption equilibrium, the solutions were filtrated and the filtrate concentrations of PDM/ZnO were determined using a UV spectrophotometer. The amount of PDM/ZnO adsorbed was calculated by subtracting the remnant PDM/ZnO concentration in the solution from the initial concentration. The quantities of PDM/ZnO adsorbed per unit amount of adsorbent (q_e) were calculated from the obtained data.

For adsorption kinetics at 25°C, the experiment was conducted in a fashion similar to that described in the experimental methods of contact time effects. All of the experiments were duplicated to check the reproducibility of data and the average values were taken.

3. Results and discussion

3.1. Material characterization

The FTIR spectrum of the PDM/ZnO is shown in Fig. 1. The bands at 1,382 and 2,924 cm^{-1} were ascribed to CH_3 and CH_2 stretching vibration, respectively. The band at 3,417 cm^{-1} was ascribed to N–H and O–H stretching vibration. The peaks at 1,722 and 1,674 cm^{-1} were assigned to C=O stretching vibration which were characteristic absorption of –COOH and $–CONH_2$ vibrations. The peak that appeared at 432 cm^{-1} was attributed to the ZnO.

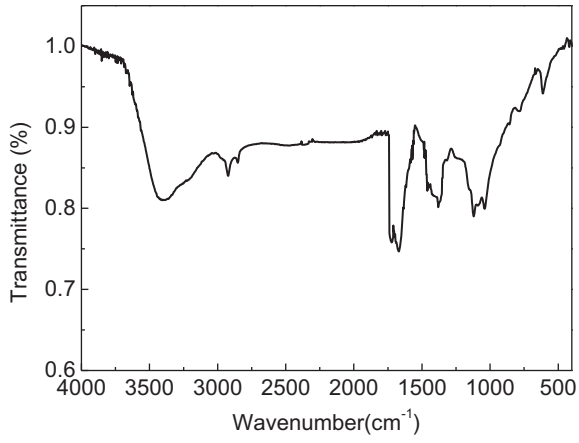

Fig. 1. The FTIR spectrum of PDM/ZnO.

3.2 Effects of contact time and initial adsorbate concentration

The uptake rates of PDM/ZnO by AS and IAS are shown in Fig. 2. The adsorption efficiency increased rapidly within the first 10 min and then slowed, approaching a steady state after 30 min. The amount of PDM/ZnO adsorbed on sludge remained almost constant from 30 to 90 min. Fig. 2 shows that maximum percent adsorption of the PDM/ZnO was after about 30 min of shaking. The rate of adsorption is higher in the beginning because of the available larger surface area of the adsorbent [27]. As a result, the equilibration time was set to 30 min for subsequent experiments.

Adsorption of PDM/ZnO on AS was carried out at different initial PDM/ZnO concentrations (50, 150, and 400 mg/L) at pH 7 and 25°C temperature. The result in Fig. 3 shows that the uptake of the PDM/ZnO increases with increasing initial PDM/ZnO

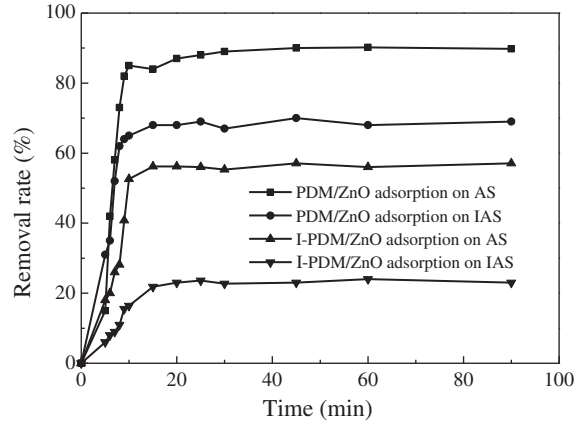

Fig. 2. Removal rates of nanocomposites by AS and IAS.

concentration. The result is in agreement with literature for the adsorption of organic substances onto AS [28,29]. The initial PDM/ZnO concentration provides the necessary driving force to overcome the resistance to the mass transfer of PDM/ZnO between the aqueous phase and the solid phase. Hence, a higher initial concentration of PDM/ZnO will enhance the adsorption process [30]. The removal amounts of PDM/ZnO with initial adsorbate concentrations at 50, 150, and 400 mg/L were found to be 44, 138, and 361 mg/g. Results show that the initial PDM/ZnO concentration played an important role in the adsorption of PDM/ZnO by AS.

3.3 Comparison of PDM/ZnO removal with AS and IAS

Fig. 2 shows the removal percentages of PDM/ZnO and I-PDM/ZnO with MLSS 1,000 mg/L of AS and IAS. The removal rates of PDM/ZnO by AS and IAS were 90.3 and 69.8%, respectively, and the removal rates for I-PDM/ZnO between AS and IAS were approximately 56 and 37%. Studies showed that the adsorption experiments were performed with AS and IAS in order to distinguish pure adsorption processes and biosorption [22,23]. Interestingly, in this study adsorption of PDM/ZnO was very fast suggested that the impact of biodegradation was neglectable. Thus, PDM/ZnO adsorbed about 20% less to IAS than to AS might be due to the different properties of the two sludges.

AS and IAS were qualitatively compared using brightfield images (Fig. 4(a0) and (b0)). AS has visible and clear surface morphology such as filaments and spheres of different sizes and loose volume. On the contrary, IAS appears as amorphous clumps of matter and lacks distinct feature. The SEM analysis gives a sufficient overview of the surface morphology and fundamental physical properties of the adsorbent. SEM images of bare AS and IAS are shown in Fig. 4(a1) and (b1). Compare with the SEM figures, the chemical activation done on AS resulted in the appearance of noticeably more pores than that on IAS. However, the entire surfaces are not seen with clear pores. The accumulation could be vaguely seen in Fig. 4(a2) and (b2) are believed to be caused by PDM/ZnO adsorption onto it. EDX spectra (Fig. 5(b)) show the appearance of additional elemental peak for Zn in AS after adsorption, which indicated the distribution of PDM/ZnO on AS surface. The surface area of AS was 1.567 m^2/g; in contrast, the surface area of IAS could not be detected by N_2 adsorption. It could be observed in the experiments that AS with NaN_3 addition leads to a smaller floc size, which is in accordance with the former study [31]. The Zeta potential of the two adsorbents had no obvious differences (Fig. 6). All these indicate that larger surface area available for adsorption and more cavities on the AS allowed easier penetration of the PDM/ZnO molecule into the adsorption sites [32–34]. The results of our batch adsorption experiments and images indicate that PDM/ZnO associate less with IAS than with AS. Therefore, IAS is not a suitable adsorbent for estimating nanoparticle removal in wastewater treatment plants.

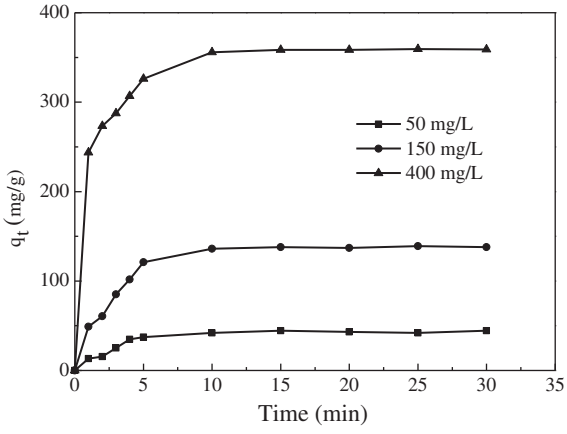

Fig. 3. Effect of initial PDM/ZnO concentration on adsorption by AS.

3.4. Effect of pH

The effect of initial pH on the removal efficiency of the AS is illustrated in Fig. 6(a). From the results, PDM/ZnO removal rate increased from 60 to 91% in the pH range of 3–8 and attained the highest value at pH 8. However, the PDM/ZnO removal rate decreased when the pH was between 9 and 12, which indicated that the removal of PDM/ZnO from aqueous solution was strongly effected by the initial pH of solution. This can be explained by the changes of physicochemical properties of the adsorbent and PDM/ZnO molecules.

The Zeta potentials of AS and PDM/ZnO are plotted in Fig. 6(a), which shows that PDM/ZnO is an amphoteric polymer. The lower adsorption at lower pH may be attributed to the presence of excess protons in solution competing with cations for the adsorption [29]. With the pH increasing from 3 to 8, the number of negative charged surface sites increases. Adsorption increases because of the increase of electrostatic attraction between negative charged biomass and positively charged PDM/ZnO molecules. Electrostatic repulsion exists between the

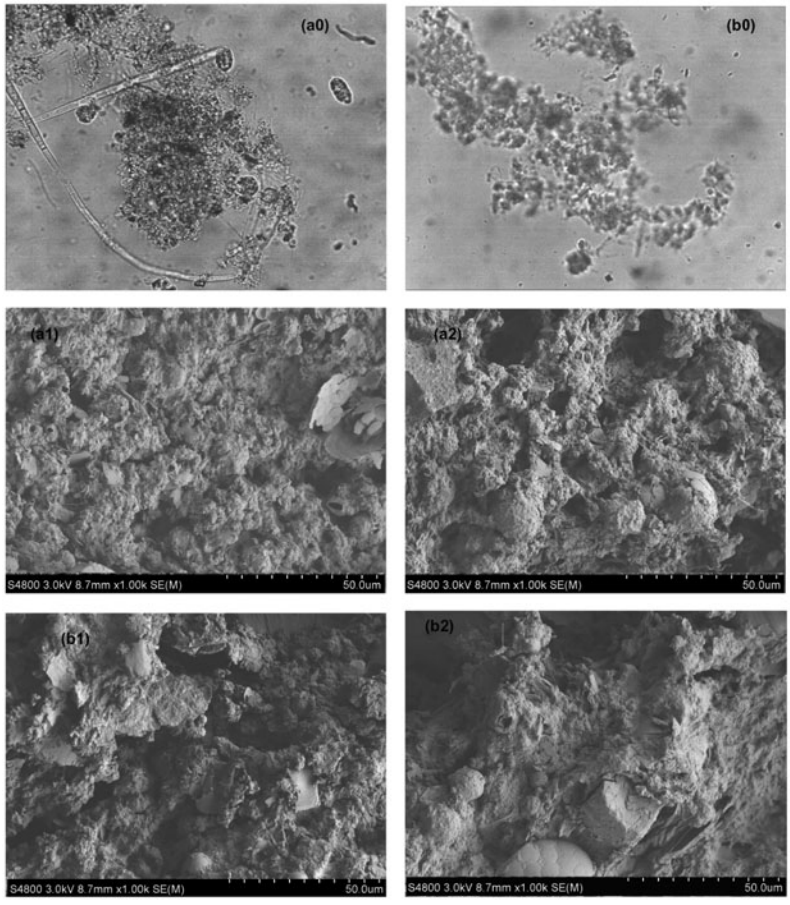

Fig. 4. Brightfield images of AS (a0), IAS (b0). SEM photographs of AS (a1), IAS (b1), PDM/ZnO adsorption on AS (a2), and IAS (b2).

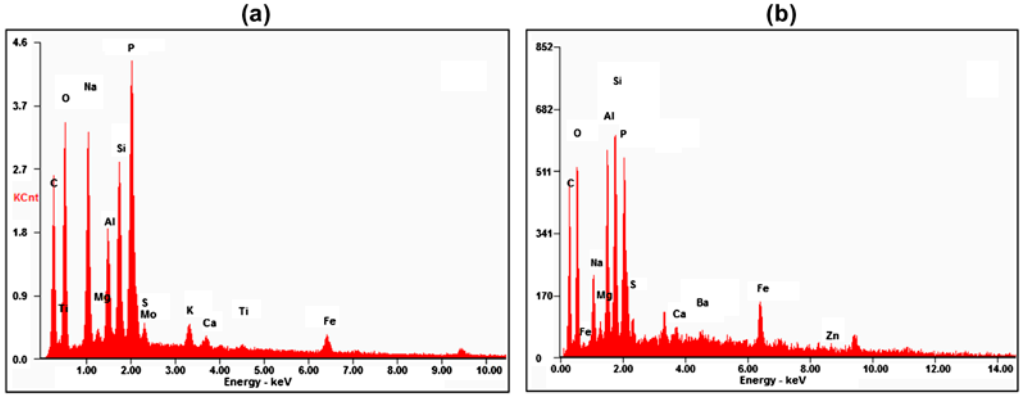

Fig. 5. EDX spectra of AS (a) before adsorption and (b) after adsorption.

negatively charged surface and negative charged PDM/ZnO molecule when the pH higher than 8. Strong dependence of PDM/ZnO adsorption on solution pH indicates that electrostatic force may

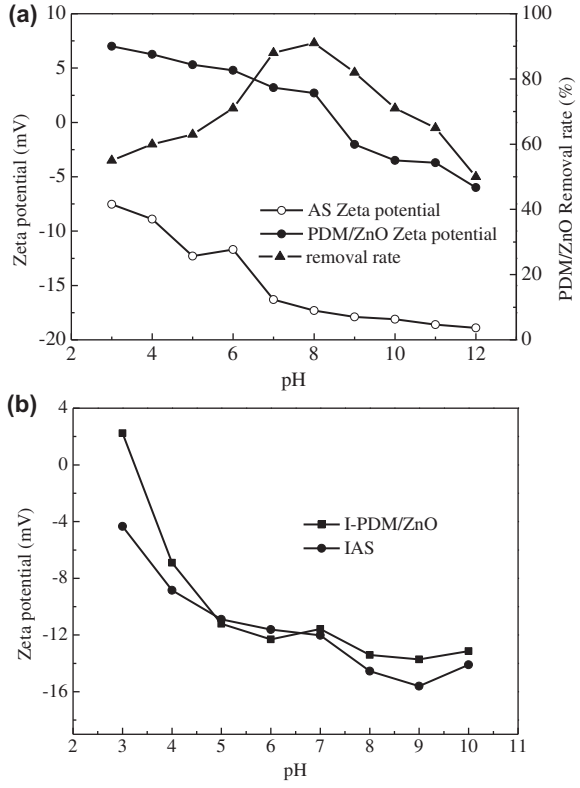

Fig. 6. Effect of initial pH on adsorption and zeta potentials of AS, and PDM/ZnO (a). Variation of Zeta potentials of IAS and I-PDM/ZnO (b).

play an important role in PDM/ZnO adsorption onto AS.

3.5 Effect of PDM/ZnO production method on adsorption

Study has found that different production methods affect nanoparticles on biosorption [17]. Adsorption experiments were carried out to investigate the effect of the preparation methods of nanocomposites on the removal of PDM/ZnO in wastewater biomass. The uptake rates of I-PDM/ZnO by AS and IAS are shown in Fig. 2. The removal rates of I-PDM/ZnO by AS and IAS were 56 and 37%, respectively. Compared with the result described in section 3.3, I-PDM/ZnO was less readily removed from AS and IAS than PDM/ZnO. Because of a different nanocomposite preparation method, the particle size of the two adsorbates have no obvious differences, the particle size distribution are all bimodal, mainly containing two particle classes, primary particles (100–140 nm), and nanoparticles (4–20 nm). PDM/ZnO has greater Zeta potential than IS-PDM/ZnO (Fig. 6), which suggests that the surface charge of PDM/ZnO could affect its removal. Increasing positive charges may result in increasing electrostatic attraction, which may increase the PDM/ZnO adsorption on AS and IAS. This further implied that electrostatic force was significant mechanism in the PDM/ZnO nanocomposite removal process. The octanol-water partition coefficients (K_{OW}) of the two nanocomposites were determined by shake flask method. PDM/ZnO has a much higher K_{OW} (28) value than that of I-PDM/ZnO (6), revealing that the hydrophobic interactions also effect nanocomposites adsorption. The finding suggests that PDM/ZnO made by free radical polymerization production method will more likely be adsorbed to AS and IAS than that made by *in situ* polymerization.

3.6. Adsorption isotherms

Adsorption isotherms of PDM/ZnO onto AS at 15, 25, and 35℃ are shown in Fig. 7. The adsorption isotherms of the PDM/ZnO on the adsorbent indicate that the adsorption capacity increase as the temperature and the equilibrium concentration of the PDM/ZnO increasing, which suggest that PDM/ZnO adsorption onto AS is favored at high temperatures and the adsorption process is endothermic. This may be the result of the increase of PDM/ZnO mobility with temperature increase. To further understand the adsorption mechanism, Langmuir (2) and Freundlich equations (3) [35] were used to fit the experimental result.

$$q_e = q_m \frac{K_L C_e}{1 + K_L C_e} \tag{2}$$

$$\log q_e = \log K_F + \frac{1}{n} \log C_e \tag{3}$$

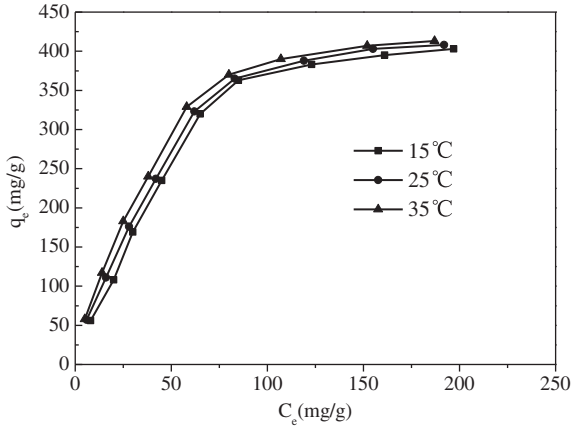

Fig. 7. Adsorption isotherms of PDM/ZnO onto AS at different temperatures.

where q_e (mg/g) is the equilibrium adsorption amount, q_m (mg/g) is the theoretical maximum adsorption capacity of adsorbent for PDM/ZnO corresponding to complete monolayer coverage, and K_L (L/mg) is the equilibrium constant related to the energy of adsorption, K_f is Freundlich constant ($mg^{1-1/n}\ L^{1/n}/g$), and $1/n$ is the heterogeneity factor.

The fitting parameters for PDM/ZnO adsorption isotherms based on Langmuir and Freundlich equations were calculated and the data are given in Table 1. The fitting results showed that the relative coefficient (R^2) of Langmuir model (0.990) was higher than that of Freundlich model, indicating that PDM/ZnO adsorption onto AS can be better fitted to the Langmuir model than Freundlich model and the adsorption of PDM/ZnO on adsorbent is a monolayer adsorption. The maximum adsorption capacity, as quantified by the Langmuir parameter q_m for AS was calculated at different temperatures (15, 25, and 35℃), and the respective values of q_m were 517, 543, and 562 mg/g.

It has been shown that n values between 1 and 10 represent good adsorption potential of the adsorbent [36]. As the temperature increased, the Freundlich constant n increased from 2.09 to 3.29, whereas K remained nearly constant. These results imply that the energy of the adsorption sites on the adsorbent has an exponential distribution [37]. The fitting results for the two equations show that the adsorption of PDM/ZnO onto AS is favorable under the study conditions.

On the basis of further analysis of the Langmuir equation, separation factor constant (R_L) is the dimensionless parameter of the equilibrium or adsorption intensity, which is widely used to describe the adsorption intensity of a surface. R_L is defined as (4):

$$R_L = \frac{1}{1 + K_L C_0} \tag{4}$$

The value of R_L indicates the shape of the isotherm to be either unfavorable ($R_L > 1$), linear ($R_L = 1$), favorable ($0 < R_L < 1$), or irreversible ($R_L = 0$) [38].

The initial concentration of the solution C_0 ranged from 50 to 600 mg/L, and the R_L values are 0.106–0.541, 0.109–0.925, and 0.0575–0.379 for PDM/ZnO adsorption at 15, 25, and 35℃, respectively. These parameters ($0 < R_L < 1$) indicate that the AS is an effective adsorbent for the adsorption of PDM/ZnO from an aqueous solution.

3.7. Adsorption kinetics

Given a heterogeneous adsorption process, the pseudo-second-order model is usually adopted to follow the mass transfer process. For pseudo-second-order kinetics, the adsorption process can be described by Eq. (5):

$$\frac{t}{q_t} = \frac{1}{k_2 q_e^2} + \frac{t}{q_e} \tag{5}$$

where q_e (mg/g) is the adsorption amount, q_t (mg/g) is the adsorption amount at time t (min), and k_2 (g/(mg·min)) is the constant of pseudo-second adsorption rate. This model is more likely to predict the kinetic behavior of adsorption [39].

Parameters were calculated from the slopes of the respective linear plots of t/q_t vs. t are given in Table 2. The relative coefficients (R^2) are higher than 0.99. The experiment equilibrium adsorption capacities ($q_{e,exp}$) are 361 and 279 mg/g in AS and IAS, respectively, which are consistent with the calculated capacity data ($q_{e,cal}$). PDM/ZnO adsorption onto AS and IAS can be well described by pseudo-second-order kinetic model. The rate constants of AS and IAS calculated are 0.0264 and 0.0168.

3.8. Thermodynamic studies

The increase in adsorption percentage with the rise in temperature was attributed to the endothermic nature of the process and was further explained by the evaluation of thermodynamic parameters. Thermodynamic parameters such as free energy change (ΔG°), enthalpy change (ΔH°), and entropy change (ΔS°) for the adsorption of PDM/ZnO on AS were determined by the application of the following Eqs. (6) and (7):

Table 1
Langmuir and Freundlich model parameters of PDM/ZnO onto AS

	Langmuir model parameters			Freundlich model parameters		
Temperature (℃)	q_m (mg/g)	K_L (L/mg)	R^2	K_f ($mg^{1-1/n}\ L^{1/n}/g$)	n	R^2
15	517	0.00841	0.997	15.48	2.09	0.954
25	543	0.014	0.993	15.50	2.13	0.927
35	562	0.0164	0.990	16.12	3.29	0.918

Table 2
Pseudo-second-order kinetic model parameters of PDM/ZnO onto AS and IAS

Adsorbent	$q_{e,exp}$ (mg/g)	$q_{e,\ cal}$ (mg/g)	k_2 (g/(mg min))	R^2
AS	361	358	0.0264	0.998
IAS	279	280	0.0168	0.999

Table 3
Thermodynamic parameters calculated for PDM/ZnO adsorption onto AS at different temperatures

	Thermodynamic parameters		
Temperature (℃)	ΔG° (kJ/mol)	ΔH° (kJ/mol)	ΔS° (kJ/(mol K))
15	−11.5	24.6	0.0454
25	−12.1		
35	−12.6		

$$\Delta G^\circ = -RT\ln K \tag{6}$$

$$\ln K = -\frac{\Delta H^\circ}{RT} + \frac{\Delta S^\circ}{R} \tag{7}$$

where R is the universal gas constant (8.314 J/(mol K)), T is the temperature (K), and K is the Langmuir constant [40]. According to Eq. (7), the ΔH° and ΔS° parameters can be calculated from the slope and intercept of the plot of $\ln K$ vs. $1/T$ yields respectively (Table 3). From Table 3, the ΔH° and ΔS° values are 24.6 kJ/mol and 45.4 J/(mol K), respectively. The positive ΔH° value means that the adsorption process is carried out as endothermic nature between 15 and 35℃ [41]. The positive ΔS° value suggests increased randomness at the solid/solution interface occurs in the internal structure of the adsorption of PDM/ZnO onto AS. The values of ΔG° for adsorption of PDM/ZnO are −11.5, −12.1, and −12.6 kJ/mol at 15, 25, and 35℃, respectively. The ΔG° values decreased with an increase in the temperature from 15 to 35℃. This reveals an increase in adsorption of PDM/ZnO with increasing temperature [42]. The negative values of ΔG° indicate that the interaction between adsorption sites and the adsorbing ion is electrostatic attraction [43]. The negative values of ΔG° also confirm the feasibility and spontaneous nature of the adsorption.

4. Conclusion

The adsorption experiments showed the effectiveness of AS in the removal of PDM/ZnO from aqueous solutions. The AS is more effective than IAS in the removal of PDM/ZnO. The effects of pH, PDM/ZnO production method, and properties of the adsorbent indicate that electrostatic force and increment of adsorbent surface area play significant roles in the removal process. Hydrophobic interactions also have impact on PDM/ZnO removal from water. The experimental data fitted with the pseudo-second-order kinetic model and Langmuir isotherm model well. AS could be used as adsorbent in removing the PDM/ZnO nanocomposite in wastewater treatment and definitely this would eliminate potential toxicity of PDM/ZnO nanocomposite on the environment.

Acknowledgments

This work was supported by 973 Program (No. 2011CB612309), Scientific Research Plan of Shaanxi Province (No. 2012K08-03), Research and Innovation Teams Plan of Shaanxi Province (2013KCT-08).

References

[1] R. Brayner, S.A. Dahoumane, C. Yéprémian, C. Djediat, M. Meyer, A. Couté, F. Fiévet, ZnO nanoparticles: Synthesis, characterization, and ecotoxicological studies, Langmuir 26 (2010) 6522–6528.
[2] R.D. Handy, F. von der Kammer, J.R. Lead, M. Hassellöv, R. Owen, M. Crane, The ecotoxicology and chemistry of manufactured nanoparticles, Ecotoxicology 17 (2008) 287–314.
[3] N.M. Franklin, N.J. Rogers, S.C. Apte, G.E. Batley, G.E. Gadd, P.S. Casey, Comparative toxicity of nanoparticulate ZnO, Bulk ZnO, and $ZnCl_2$ to a freshwater microalga (*Pseudokirchneriella subcapitata*): The importance of particle solubility, Environ. Sci. Technol. 41 (2007) 8484–8490.

[4] Y. Liu, L. He, A. Mustapha, H. Li, Z.Q. Hu, M. Lin, Antibacterial activities of zinc oxide nanoparticles against *Escherichia coli* O157:H7, J. Appl. Microbiol. 107 (2009) 1193–1201.
[5] M. Li, L.Z. Zhu, D.H. Lin, Toxicity of ZnO nanoparticles to *Escherichia coli*: Mechanism and the influence of medium components, Environ. Sci. Technol. 45 (2011) 1977–1983.
[6] R. Brayner, R. Ferrari-Iliou, N. Brivois, S. Djediat, M.F. Benedetti, F. Fiévet, Toxicological impact studies based on *Escherichia coli* bacteria in ultrafine ZnO nanoparticles colloidal medium, Nano Lett. 6 (2006) 866–870.
[7] V. Aruoja, H.C. Dubourguier, K. Kasemets, A. Kahru, Toxicity of nanoparticles of CuO, ZnO and TiO_2 to microalgae *Pseudokirchneriella subcapitata*, Sci. Total Environ. 407 (2009) 1461–1468.
[8] S.W.Y. Wong, P.T.Y. Leung, A.B. Djurišić, K.M.Y. Leung, Toxicities of nano zinc oxide to five marine organisms: Influences of aggregate size and ion solubility, Anal. Bioanal. Chem. 396 (2010) 609–618.
[9] D.H. Lin, B.S. Xing, Root uptake and phytotoxicity of ZnO nanoparticles, Environ. Sci. Technol. 42 (2008) 5580–5585.
[10] P. Miralles, T.L. Church, A.T. Harris, Toxicity, uptake, and translocation of engineered nanomaterials in vascular plants, Environ. Sci. Technol. 46 (2012) 9224–9239.
[11] M.A. Kiser, D.A. Ladner, K.D. Hristovski, P.K. Westerhoff, Nanomaterial transformation and association with fresh and freeze-dried wastewater activated sludge: Implications for testing protocol and environmental fate, Environ. Sci. Technol. 46 (2012) 7046–7053.
[12] A. Tartakovsky, D.M. Drutis, J.O. Carnali, The adsorption of cationic and amphoteric copolymers on glass surfaces: Zeta potential measurements, adsorption isotherm determination, and FT Raman characterization, J. Colloid Interface Sci. 263 (2003) 408–419.
[13] S.A. Asrof, A.A.M. Hasan, Participation of propargylmoiety in Butler's cyclopolymerization process, Polymer 45 (2004) 8097–8107.
[14] C. Wandrey, J. Hernndez-Barajas, D. Hunkeler, Diallyldimethylammonium chloride and its polymers, Adv. Polym. Sci. 145 (1999) 123–128.
[15] Y.H. Chen, A. Lin, F.X. Gan, Improvement of polyacrylate coating by filling modified nano-TiO, Appl. Surf. Sci. 252 (2006) 8635–8640.
[16] Y. Li, D.G. Gao, J.Z. Ma, B. Lv, Synthesis of vinyl polymer/ZnO nano composite and its application in leather tanning agent, Mater. Sci. Forum 694 (2011) 103–107.
[17] M.A. Kiser, H. Ryu, H. Jang, K. Hristovski, P. Westerhoff, Biosorption of nanoparticles to heterotrophic wastewater biomass, Water Res. 44 (2010) 4105–4114.
[18] G. Byrns, The fate of xenobiotic organic compounds in wastewater treatment plants, Water Res. 35 (2001) 2523–2533.
[19] D. Dionisi, L. Bornoroni, S. Mainelli, M. Majone, F. Pagnanelli, M.P. Papini, Theoretical and experimental analysis of the role of sludge age on the removal of adsorbed micropollutants in activated sludge processes, Ind. Eng. Chem. Res. 47 (2008) 6775–6782.
[20] H. Melcer, P. Steel, W.K. Bedford, Removal of polycyclic aromatic hydrocarbons and heterocyclic nitrogen compounds in a municipal treatment plant, Water Environ. Res. 67 (1995) 926–934.
[21] Fate, Transport and Transformation Test Guidelines: OPPTS 835.1110 Activated Sludge Sorption Isotherm. EPA 712-C-98-298, United States Environmental Protection Agency, Washington, DC, 1998.
[22] Y.H. Wu, J.Z. He, L.Z. Yang, Evaluating adsorption and biodegradation mechanisms during the removal of Microcystin-RR by periphyton, Environ. Sci. Technol. 44 (2010) 6319–6324.
[23] B. Li, T. Zhang, Biodegradation and adsorption of antibiotics in the activated sludge process, Environ. Sci. Technol. 44 (2010) 3468–3473.
[24] D. Saisho, M. Nakazono, N. Tsutsumi, A. Hirai, ATP synthesis inhibitors as well as respiratory inhibitors increase steady-state level of alternative oxidase mRNA in *Arabidopsis thaliana*, J. Plant Physiol. 158 (2001) 241–245.
[25] M. Clara, B. Strenn, E. Saracevic, N. Kreuzinger, Adsorption of bisphenol-A, 17β-estradiole and 17α -ethinylestradiole to sewage sludge, Chemosphere 56 (2004) 843–851.
[26] B. Samiey, A. Toosi, Adsorption of malachite green on silica gel: Effects of NaCl, pH and 2-propanol, J. Hazard. Mater. 184 (2010) 739–745.
[27] J. Rahchamani, H. Zavvar Mousavi, M. Behzad, Adsorption of methyl violet from aqueous solution by polyacrylamide as an adsorbent: Isotherm and kinetic studies, Desalination 267 (2011) 256–260.
[28] M. Chio, H. Li, Adsorption behavior of reactive dye in aqueous solution on chemical cross-linked chitosan beads, Chemosphere 50 (2003) 1095–1105.
[29] O. Gulnaz, A. Kaya, S. Dincer, The reuse of dried activated sludge for adsorption of reactive dye, J. Hazard. Mater. 134 (2006) 190–196.
[30] R. Ren, D.F. Liu, X.K. Li, J. Sun, C. Zhang, Adsorption of quaternary ammonium compounds onto activated sludge, Water Resour. Prot. 3 (2011) 105–113.
[31] E. Barbot, I. Seyssiecq, N. Roche, B. Marrot, Inhibition of activated sludge respiration by sodium azide addition: Effect on rheology and oxygen transfer, Chem. Eng. J. 163 (2010) 230–235.
[32] Y.S. Ho, G. McKay, D.A.J. Wase, C.F. Forster, Study of the sorption of divalent metal ions on to peat, Adsorpt. Sci. Technol. 18 (2000) 639–650.
[33] J.W.T. Wimpenny, R. Colasanti, A unifying hypothesis for the structure of microbial biofilms based on cellular automaton models, FEMS Microbiol. Ecol. 22 (1997) 1–16.
[34] L.J. Scinto, K.R. Reddy, Biotic and abiotic uptake of phosphorus by periphyton in a subtropical freshwater wetland, Aquat. Bot. 77 (2003) 203–222.
[35] O. Altin, H.Ö. Özbelge, T. Dogu, Use of general purpose adsorption isotherms for heavy metal–clay mineral interactions, J. Colloid Interface Sci. 198 (1998) 130–140.
[36] E. Errais, J. Duplay, F. Darragi, I. M'Rabet, A. Aubert, F. Huber, G. Morvan, Efficient anionic dye adsorption on natural untreated clay: Kinetic study and thermodynamic parameters, Desalination 275 (2011) 74–81.

[37] A. Sar, G. Sahinoglu, M. Tuzen, Antimony(III) adsorption from aqueous solution using raw perlite and Mn-modified perlite: Equilibrium, thermodynamic, and kinetic studies, Ind. Eng. Chem. Res. 51 (2012) 6877–6886.
[38] T.W. Weber, P.K. Chakravorti, Pore and solid diffusion models for fixed adsorbers, J. Am. Inst. Chem. Eng. 20 (1974) 226–237.
[39] L.K. Wang, M.H. Wang, R.C. Ziegler, Quaternary ammonium thickening of sewage sludge in magnetic field, Ind. Eng. Chem. Prod. Res. Dev. 16 (1977) 311–315.
[40] C.P. Wang, J.T. Liu, Z.Y. Zhang, B.L. Wang, H.W. Sun, Adsorption of Cd(II), Ni(II), and Zn(II) by Tourmaline at acidic conditions: Kinetics, thermodynamics, and mechanisms, Ind. Eng. Chem. Res. 51 (2012) 4397–4406.
[41] H. Tang, W.J. Zhou, L. Zhang, Adsorption isotherms and kinetics studies of malachite green on chitin hydrogels, J. Hazard. Mater. 209–210 (2012) 218–225.
[42] S. Khattria, M. Singh, Removal of malachite green from dye wastewater using neem sawdust by adsorption, J. Hazard. Mater. 167 (2009) 1089–1094.
[43] K. Gobi, M.D. Mashitah, V.M. Vadivelu, Adsorptive removal of Methylene Blue using novel adsorbent from palm oil mill effluent waste activated sludge: Equilibrium, thermodynamics and kinetic studies, Chem. Eng. J. 171 (2011) 1246–1252.